Available online at www.sciencedirect.com
ScienceDirect
Procedia Computer Science 1 (2010) 811–818
Procedia Computer Science
www.elsevier.com/locate/procedia

International Conference on Computational Science, ICCS 2010

Lattice Boltzmann model for simulation of the electric breakdown in liquids

D.A. Medvedev

Interdisciplinary Centre for Advanced Materials Research (ICAMS), Ruhr University Bochum, Stiepeler Str. 129, 44780, Bochum, Germany
Lavrentyev Institute of Hydrodynamics, Siberian Branch of Russian Academy of Sciences, Lavrentyev prosp. 15, 630090, Novosibirsk, Russia

Abstract

We investigate pre-breakdown hydrodynamic flows and initial stages of the electric breakdown in dielectric liquids. Three models are considered. The first one represents the purely thermal mechanism. Here, the liquid is simulated by a single-phase lattice Boltzmann equation (LBE) method. The temperature and the electric charge density are described by additional LBE components with zero mass. The permittivity is assumed to be constant. The conductivity increases with the increase of temperature. Electric force acting on a charged liquid is coupled with the hydrodynamics by the exact difference method [Kupershtokh, 2004; Kupershtokh & Medvedev, J. Electrostatics, 2006]. The last process in the model is the Joule heating.

In the second model, a possible phase transition is included. To simulate a fluid with an arbitrary two-phase equation of state (such as van der Waals or Carnahan-Starling EOS), the method proposed by Kupershtokh is used [Kupershtokh, 2005; Kupershtokh et al., 2007]. The conductivity increases with the decrease of the fluid density. When the voltage is applied, the charge injection from the surface of electrode begins. The electric force acting on the charged fluid produces negative pressure near electrode leading to a phase transition (evaporation). Conductivity increases leading to enhanced evaporation and growth of a conducting bubble. Thus, the bubble mechanism of breakdown is realized.

The last model includes the density-dependent permittivity. For nonpolar liquids, the dependence is given by the Clausius – Mosotti law. In this case, several additional processes are possible. First, dielectrics is pulled into regions with higher electric field which produces rarefaction waves. Second, an anisotropic instability [Kupershtokh & Medvedev, Phys. Rev. E, 2006] can develop producing low-density channels along the electric field. Since these channels can easily become conducting, another mechanism of the breakdown is realized.

Keywords: Electric breakdown of liquids; Lattice Boltzmann equation method; Phase transition; Two-phase flow
PACS: 77.22.Jp, 83.10.Rs, 64.70.F-, 47.20.Hw

1. Introduction

Electric breakdown of liquids is an interesting and important phenomenon for the science and the industry. From the scientific point of view, it is first of all an interdisciplinary phenomenon, including electrodynamics, hydrodynamics, thermophysics, physics of plasma and so on.

Email address: dmedv@hydro.nsc.ru (D.A. Medvedev)
1877-0509
doi:10.1016/j.procs.2010.04.088

Unlike the breakdown of solids, in the case of liquid, electrohydrodynamic flows play an important role. Such flows are formed under the action of electric field. On the other hand, charge transfer and change of the electric permittivity influence the distribution of the electric potential. To make the situation even more complicated, phase boundaries between liquid, vapor and plasma can appear and disappear in the bulk of a fluid. The range of characteristic scales is large, from the streamer channels width of order of 10 micrometers to the interelectrode gap which can be as large as 10 cm.

Early simulations of the electric breakdown of liquids dealt mainly with the inception and propagation of streamers. Niemeyer, Pietronero and Wiesmann assumed the streamer structure to be equipotential [6]. Later, the charge relaxation was taken into account, and different breakdown criteria were proposed [7, 8, 9, 10]. Several such models were compared in the paper [11]. In all these works, the flow of liquid was neglected.

The expansion of streamer channels was taken into account in the model proposed in [12]. The pressure inside channels was calculated using a simple approximate model. The influence of the flow on conductive channels was neglected. Propagation of a positive streamer in liquid argon was simulated in [13]. Here, only the dynamics of ionization and recombination was considered, and the density of liquid was assumed constant. Lattice gas and lattice Boltzmann method were first applied to investigate the dynamics of streamers in dielectric liquid in [14].

Mesoscopic methods such as the multiphase LBE method are especially suitable for simulation of such flows because they provide unified description of all transport processes and allow one to avoid tracking the interphase boundaries.

The paper is organized as follows. In Sec. 2, we describe the mathematical model. In Sec. 3, the details of the numerical method are described. The simulation results are given in Sec. 4 where we discuss three models: the simplest thermal model, the bubble model, and the combined model. Some concluding remarks are given in Sec. 5.

2. Model equations

Here, we list the governing equation for the system under investigation. First, the hydrodynamics of a fluid is described by the continuity equation

$$\frac{\partial \rho}{\partial t} + \operatorname{div}(\rho \mathbf{u}) = 0, \tag{1}$$

and the Navier-Stokes equation

$$\frac{\partial \rho \mathbf{u}}{\partial t} + \operatorname{div} \Pi^{(0)}_{\alpha\beta} = \mathbf{F} + \eta \Delta \mathbf{u} + \left(\eta + \frac{\zeta}{3}\right) \nabla \operatorname{div} \mathbf{u}. \tag{2}$$

Here, ρ is the fluid density, $\mathbf{u}$ is the mass velocity, $\Pi^{(0)}_{\alpha\beta} = P\delta_{\alpha\beta} + \rho u_\alpha u_\beta$ is the nonviscous part of the momentum flux tensor, η is the dynamic viscosity of the fluid, ζ is the second viscosity coefficient. The force $\mathbf{F}$ arises due to the interparticle interaction, and the action of the electric field on the charged fluid.

The electric part of the problem is described by the equation of the charge transport

$$\frac{\partial q}{\partial t} + \operatorname{div}(q\mathbf{u}) = D\Delta q - \operatorname{div}(\sigma \mathbf{E}), \tag{3}$$

where q is the charge density, D is the charge diffusivity, σ is the fluid conductivity which can depend on the density and temperature, $\mathbf{E}$ is the electric field. This equation describes the convective charge transport, the charge diffusion, and the conductivity current. The distribution of the electric potential φ and the electric field $\mathbf{E}$ can be found from the Poisson's equation

$$\operatorname{div}(\varepsilon \nabla \varphi) = -4\pi q, \ \mathbf{E} = -\nabla \varphi. \tag{4}$$

The body force acting on charged dielectric liquid in an electric field is given by the Helmholtz formula [15]

$$\mathbf{F} = q\mathbf{E} - \frac{E^2}{8\pi} \nabla \varepsilon + \frac{1}{8\pi} \nabla \left[E^2 \rho \left(\frac{\partial \varepsilon}{\partial \rho} \right)_T \right]. \tag{5}$$

The second and third terms represent the action of electric field on polarization charges in nonuniform dielectric and the electrostriction force.

The last part of the model is the equation of heat transport

$$\frac{\partial T}{\partial t} + \mathrm{div}\,(T\mathbf{u}) = \chi \Delta T + Q. \tag{6}$$

Here, χ is the thermal diffusivity. The last term represents the Joule heating which is equal to $Q = \sigma E^2/c_p$, c_p is the specific heat. To close the system of equations, we should provide the equation of state for the fluid, and the temperature and density dependence of the conductivity σ.

3. Numerical method

The system of equations is rather large and interconnected. In order to solve it numerically, we apply the method of splitting on physical processes which was originally proposed by Yanenko [16]. In this method, the whole time step is divided into several stages implemented sequentially. These stages correspond to different physical processes which are in our case:

1. the modeling of hydrodynamic flows,
2. simulation of the convective transport and diffusion of charge carriers and heat,
3. calculation of electrostatic forces acting on a fluid,
4. calculation of the electric potential and electric currents,
5. simulation of possible phase transitions,
6. simulation of the electric breakdown, that is, the generation of conductive phase.

The hydrodynamic flow is modeled using the lattice Boltzmann method with BGK collision operator. The evolution equations for single-particle distribution functions N_k have the form

$$N_k(\mathbf{x} + \mathbf{c}_k\Delta t, t + \Delta t) = N_k(\mathbf{x}, t) + \left(N_k^{eq}(\rho, \mathbf{u}) - N_k(\mathbf{x}, t)\right)/\tau + \Delta N_k, \tag{7}$$

where $\mathbf{c}_k$ are the lattice velocities, Δt is the time step. The fluid density is $\rho = \sum N_k$, the momentum is $\rho\mathbf{u} = \sum N_k\mathbf{c}_k$. The last term ΔN_k represents the change of distribution functions due to an action of body forces. It is calculated using the exact difference method [1, 2] as the difference of equilibrium distribution functions corresponding to the same density and the mass velocities before and after the action of force

$$\Delta N_k = N_k^{eq}(\rho, \mathbf{u} + \Delta\mathbf{u}) - N_k^{eq}(\rho, \mathbf{u}). \tag{8}$$

Here, $\Delta\mathbf{u}$ is equal to $\Delta\mathbf{u} = \mathbf{F}\Delta t/\rho$. The kinematic viscosity is defined by the reduced relaxation time τ as $\nu = \left(h^2/3\Delta t\right)(\tau - 1/2)$, where h is the lattice spacing which is usually assumed to be unity. We used the standard D2Q9 model on a square lattice.

To simulate the convective transport and diffusion of charge carriers and heat, the method of additional LB component with zero mass (passive scalar) was applied [2] similar to one used in [17]. Evolution equations for the distribution functions for charge carriers are

$$q_k(\mathbf{x} + \mathbf{c}_k\Delta t, t + \Delta t) = q_k(\mathbf{x}, t) + \left(q_k^{eq}(q, \mathbf{v}) - q_k(\mathbf{x}, t)\right)/\tau_q. \tag{9}$$

The electric charge density is $q = \sum q_k$. The charge diffusivity is equal to $D = \left(h^2/3\Delta t\right)(\tau_q - 1/2)$. Equations for the heat convection are

$$T_k(\mathbf{x} + \mathbf{c}_k\Delta t, t + \Delta t) = T_k(\mathbf{x}, t) + \left(T_k^{eq}(T, \mathbf{v}) - T_k(\mathbf{x}, t)\right)/\tau_T + Q_k\Delta t \tag{10}$$

with the temperature equal to $T = \sum T_k$. The heat diffusivity is calculated as $\chi = \left(h^2/3\Delta t\right)(\tau_T - 1/2)$. Equilibrium distribution functions q_k^{eq}, T_k^{eq} depend on the hydrodynamic velocity $\mathbf{v}$ defined as $\mathbf{v} = \mathbf{u} + \Delta\mathbf{u}/2$.

The electric force acting on the liquid (5) is calculated using standard finite-difference approximation, and it is coupled with the hydrodynamics by the formula (8).

The Poisson's equation (4) is solved together with the equation of the conductive charge transport

$$\frac{\partial q}{\partial t} + \mathrm{div}\,(\sigma\mathbf{E}) = 0 \tag{11}$$

using a time-implicit finite-difference scheme proposed in [11]. Joule heating is calculated from the known electric field along a lattice link connecting nodes i and j and the link conductivity σ_{ij} which is equal to the geometric mean of nodes' conductivities, $\sigma_{ij} = \sqrt{\sigma_i \sigma_j}$. The electric breakdown is simulated by defining the temperature and density dependence of the conductivity. The threshold-type dependencies are chosen in order to describe abrupt change of the matter state.

The phase transitions are simulated by an introduction of special forces between neighbor nodes. To ensure the global momentum conservation, these forces should be equal to the gradient of special potential U. Zhang and Chen proposed [18] to express this potential using the equation of state

$$U = P(\rho, T) - \rho\theta. \tag{12}$$

Here, $\theta = h^2/\Delta t$ is the "kinetic temperature" of the LBE pseudoparticles. The correct form of the numerical approximation of the force is crucially important for the stability and the accuracy of calculations [3, 19]. We use the approximation proposed by Kupershtokh [3, 4]. There, a new function Φ was introduced

$$\Phi(\rho, T) = \sqrt{-U}, \tag{13}$$

and the force is expressed as

$$\mathbf{F} = \frac{1}{\alpha h}\left[(1-2A)\Phi(\mathbf{x})\sum_k \frac{G_k}{G_0}\Phi(\mathbf{x}+\mathbf{e}_k)\mathbf{e}_k + \sum_k \frac{G_k}{G_0}\Phi^2(\mathbf{x}+\mathbf{e}_k)\mathbf{e}_k\right]. \tag{14}$$

Here, α is a numerical coefficient depending on the lattice used. For D2Q9 model, it is $\alpha = 3/2$. Lattice vectors $\mathbf{e}_k$ are equal to $\mathbf{e}_k = \mathbf{c}_k \Delta t$. Coefficients G_k/G_0 are introduced in order to obtain isotropy. In the D2Q9 model, $G_k/G_0 = 1$ for the nearest neighbors, and $G_k/G_0 = 1/4$ for the diagonal directions. The coefficient A provides the "fine-tuning" of the coexistence curve in simulations, it depends on the equation of state used.

We used in our simulations the van der Waals equation of state in non-dimensional form

$$\tilde{P} = \frac{8\tilde{\rho}\tilde{T}}{3-\tilde{\rho}} - 3\tilde{\rho}^2 \tag{15}$$

Non-dimensional parameters are $\tilde{P} = P/P_c$, $\tilde{\rho} = \rho/\rho_c$, $\tilde{T} = T/T_c$. Here, P_c is the critical pressure, ρ_c is the critical density, T_c is the critical temperature of the fluid. The non-dimensional expression for the potential of eq. (12) is

$$\tilde{U} = k\tilde{P}(\tilde{\rho}, \tilde{T}) - \tilde{\rho}\tilde{\theta}. \tag{16}$$

Below, we drop tildes for brevity. For this equation of state, the value $A = -0.152$ gives the best agreement between theory and LBE calculations, it was used in simulations.

The coefficient $k = P_c \Delta t^2 / \left(\rho_c \Delta h^2\right)$ should be introduced in order to match physical and lattice units [4, 19]. For example, if we take $h/\Delta t = 1$ km/s, then for argon we obtain k of order of 0.01. For other inert gases, the values of k are of the same order.

4. Results

We consider three models: the pure thermal model which is the simplest one, the more elaborated bubble model, and the combined model. Below, we describe the details of each model and show the results obtained.

4.1. Thermal model

Here, the conductivity depends on the temperature through an Arrhenius law

$$\sigma = \sigma_0 \exp(-A/T) \text{ for } T > T_*. \tag{17}$$

Such dependence can arise if charge carriers are generated by a thermal ionization. If temperature is lower than the threshold value T_*, the conductivity was assumed zero. To simplify the model, no phase transition was taken into

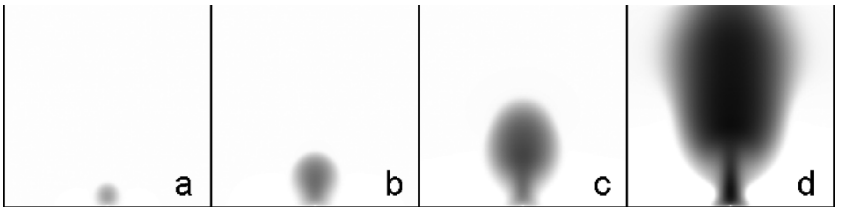

Figure 1: Growth of conductive channel. Time is t = 240 (a), 400 (b), 560 (c), 720 (d). Dark color corresponds to higher temperature

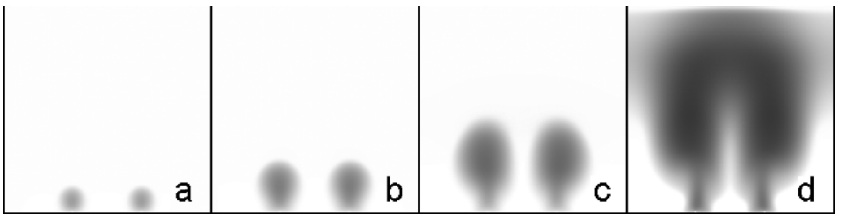

Figure 2: Growth of two conductive channels. Ratio of charge injection rates is equal to 1. Time is t = 260 (a), 400 (b), 540 (c), 680 (d). Dark color corresponds to higher temperature

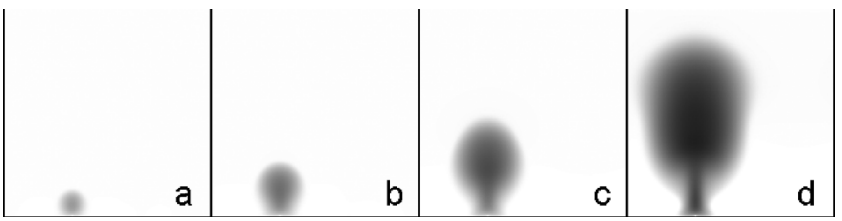

Figure 3: Growth of conductive channels. Ratio of charge injection rates is equal to 3. Time is t = 260 (a), 400 (b), 540 (c), 680 (d). Dark color corresponds to higher temperature

account. In all simulations, the electric field was directed vertically. We used periodic boundary conditions at the sides of the computation area, and solid walls at top and bottom.

Simulation results are shown in Fig. 1. The average electric field was $E_a = 0.04$, the conductivity $\sigma_0 = 0.15$, the threshold value $T_* = 0.02$, the specific heat $c_p = 0.001$, the initial temperature was zero. In the middle of the lower electrode, a small protrusion was set with a conductive layer above it. After the voltage application at $t = 0$, the charge injection from the protrusion began heating the adjacent fluid. The charged region moved to the opposite electrode under the action of electric field and expanded due to the Joule heating. At last, the conductive channel reached the second electrode, and the channel stage of the electric breakdown would begin.

In reality, many tips usually exist from which the discharge can start. In Fig. 2, the competition of breakdown from two tips is shown. Here, the conductivity near both tips was the same, other parameters are equal to those of Fig. 1. Two conductive plumes developed in parallel and overlaped at last.

In the next simulation, the conductivity near the right tip was three times lower than the conductivity near the left one. In this case, the discharge from easily-injecting tip completely screened the second tip, from which no noticeable injection occured (Fig. 3).

4.2. Bubble model

The next model can be called the bubble model. Here, the conductivity depends on the fluid density as

$$\sigma = \sigma_0(\rho_0/\rho - 1) \text{ for } \rho < \rho_*. \tag{18}$$

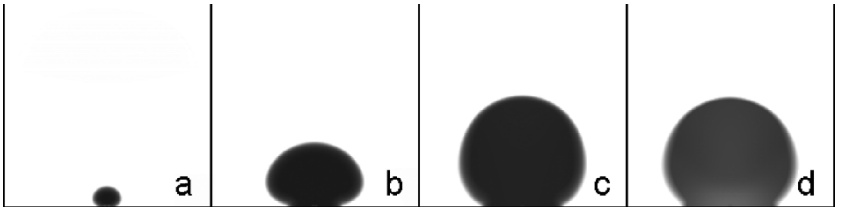

Figure 4: Growth of conductive bubble. Time is t = 180 (a), 420 (b), 660 (c), 900 (d). Dark color corresponds to lower fluid density

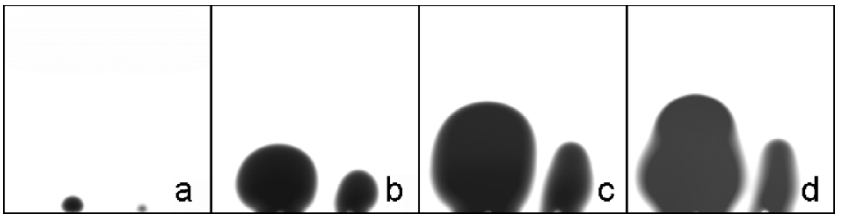

Figure 5: Growth of conductive bubble. Time is t = 200 (a), 540 (b), 880 (c), 1220 (d). Dark color corresponds to lower fluid density

This dependence reflects the fact that the mean free path of charge carriers is approximately inversely proportional to the density. Electric permittivity is assumed to be constant. Phase transitions are described by using the van der Waals EOS for the fluid in the reduced form (eq. (15)), and the coefficient $k = 0.01$.

The development of discharge in a tip-plane geometry is shown in Fig. 4. The average electric field was $E_a = 0.1$, the conductivity $\sigma_0 = 0.1$, the initial density $\rho_0 = 1.8$, the threshold value $\rho_* = 1.69$, the specific heat $c_p = 3 \cdot 10^{-4}$, the initial temperature $T_0 = 0.9$. The charge injection from the tip led to the heating of the nearby liquid, and a vapor bubble began to grow. The conductivity inside the bubble increased leading to more heating and further bubble growth. Since the boundary conditions at left and right sides were periodic, in this simulation we had a sort of a closed cell. Therefore, the overall pressure increased with time, and the bubble stoped to grow and can decay later. If we have several tips, the collective effects arise. In Fig. 5, the ratio of injection rates was 2. In this case, two bubbles developed simultaneously. Compression waves generated at the bubble expansion led to their mutual repulsion. The bubble grown near the easily-injecting tip suppressed the bubble growth from another tip.

4.3. Combined model

The force (5) acting on a dielectric fluid in electric field can lead to instability when the density dependence of permittivity is non-linear. It was shown in [5] that this instability is anisotropic, the increment for the stratification along the field is larger than for the transversal stratification. Thus, anisotropic separation into liquid and vapor phases is possible in high electric fields for a fluid that is initially in unstable state, as well as in metastable or stable states. It is important that new regions of low density phase appear as narrow cylindrical channels oriented on average along the electric field. In these channels, electric discharge can develop.

Density dependence of the electric permittivity was described by the Clausius – Mosotti law

$$\varepsilon = 1 + 3\beta\rho/(1 - \beta\rho) \tag{19}$$

which is valid for non-polar dielectrics. The coefficient β was set equal to 0.057, it is the characteristic value for argon.

The development of the anisotropic decay of dielectric liquid under action of strong electric field is shown in Fig. 6. The van der Waals EOS (15) was used, the coefficient k was $k = 0.00915$. Initial density was $\rho_0 = 1.8$, initial temperature $T_0 = 0.9$, these values correspond to a stable liquid state. The non-dimensional electric field squared was

$$\tilde{E}^2 = \frac{E^2}{8\pi P_c} = 100.$$

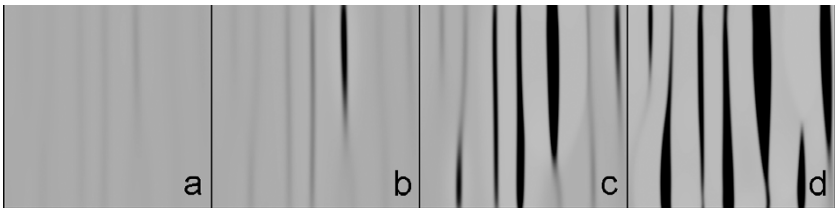

Figure 6: Anisotropic decay of the dielectric liquid in strong electric field. Time is t = 540 (a), 660 (b), 780 (c), 900 (d). Dark color corresponds to lower fluid density

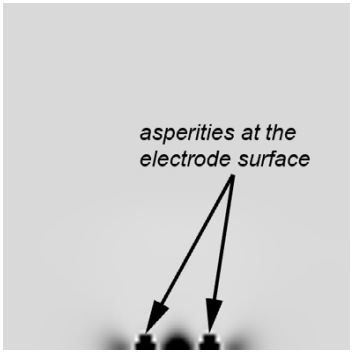

Figure 7: Formation of breakdown precursor. Non-dimensional electric field is $\tilde{E}^2 = 30$

Since this value is above the instability threshold, formation of vapor channels in a liquid began. These channels are oriented mainly along the average electric field, they have approximately round cross-section. Later, vapor channels can serve as paths for the discharge development.

The value of $\tilde{E}^2 = 100$ corresponds to extremely strong electric fields which are not achieved in experiments. To go closer to the reality, we consider the rough structure of real electrodes. In the simulation shown in Fig. 7, there were two small asperities at the surface of one electrode close together. When the voltage was applied, two rarefaction waves were formed because dielectrics was pulled to the regions of higher field. The waves met generating a region with low density between asperities. Here, dark color corresponds to higher values of E/ρ. This is a usual measure for the electric breakdown inception probability. Interestingly, the highest value was achieved not near the tips, but between them, and this value is an order of magnitude larger than without asperities. Such effect can be a new mechanism of the breakdown inception.

Lewis proposed in [20] another mechanism of streamer growth was proposed that assumed the fast propagation of Griffith crack (similar to brittle material) in a liquid containing population of initial submicroscopic spherical holes (bubbles). However, only the linear density dependence of permittivity was considered, for which the anisotropic instability of a stable or metastable state is impossible.

5. Conclusions

In conclusion, we propose a LB-based model for simulating the pre-breakdown hydrodynamic flows and initial stages of the electric breakdown in dielectric liquids. Three models were considered: the thermal model, the bubble model, and the combined model.

In the thermal model, the conductive channel moves to the opposite electrode under the action of electric field and expands due to the Joule heating. When this channel reaches the second electrode, the channel stage of the electric breakdown begins. In the case of two tips with the same injection rate, two conductive plumes grow in parallel and overlap at the last stage. When the injection rates differ significantly, the discharge from easily-injecting tip screens the second one and only one channel develops.

In the bubble model, evaporation of the liquid begins near the injecting tip due to both the heating and the electric stress. Conductivity inside the bubble increases leading to further heating and the bubble growth. When there are two tips, two bubbles grow simultaneously. Each generates the compression waves in the liquid which leads to the repulsion of bubbles. Again the bubble from easily-injecting tip suppresses the growth of another one.

With a nonlinear density dependence of the permittivity, the instability of a dielectric fluid in sufficiently high electric field can arise leading to the formation of cylindrical vapor channels in a liquid oriented on average along the electric field. Since the electric strength in a vapor is lower than in a liquid, electric discharge can develop along these channels. When there are asperities at the surface of an electrode, rarefaction waves are generated leading to the formation of a low density region between the asperities. In this region, the value of E/ρ can be an order of magnitude larger than in the case of smooth electrodes. Such effect can be a new mechanism of the breakdown inception.

The method proposed is relatively simple and it can be used to simulate a variety of pre-breakdown flows with possible phase transitions and initial stages of the electric breakdown of liquids.

References

[1] A. L. Kupershtokh, New method of incorporating a body force term into the lattice Boltzmann equation, in: Proc. 5th International EHD Workshop, University of Poitiers, Poitiers, France, 2004, pp. 241–246.
[2] A. L. Kupershtokh, D. A. Medvedev, Lattice Boltzmann method in electrohydrodynamic problems, Journal of Electrostatics 64 (7–9) (2006) 581–585.
[3] A. L. Kupershtokh, Simulation of flows with liquid-vapor interfaces by the lattice Boltzmann method, Vestnik NGU (Quart. J. of Novosibirsk State Univ.), Series: Math., Mech. and Informatics 5 (3) (2005) 29–42, [in Russian].
[4] A. L. Kupershtokh, D. I. Karpov, D. A. Medvedev, C. Stamatelatos, V. P. Charalambakos, E. C. Pyrgioti, D. P. Agoris, Stochastic models of partial discharge activity in solid and liquid dielectrics, IET Sci. Meas. Technol. 1 (6) (2007) 303–311.
[5] A. Kupershtokh, D. Medvedev, Anisotropic instability of a dielectric liquid in a strong uniform electric field: Decay into a two-phase system of vapor filaments in a liquid, Physical Review E 74 (2) (2006) 021505.
[6] L. Niemeyer, L. Pietronero, H. Wiesmann, Fractal dimension of dielectric breakdown, Physical Review Letters 52 (12) (1984) 1033–1036.
[7] A. Kupershtokh, Fluctuation model of the breakdown of liquid dielectrics, Soviet Technical Physics Letters 18 (10) (1992) 647–649.
[8] P. Biller, Fractal streamer models with physical time, in: Proc. 11^{th} Int. Conf. on Conduction and Breakdown in Dielectric Liquids, IEEE N 93CH3204-5, Baden-Dättwil, Switzerland, 1993, pp. 199–203.
[9] H. Jones, E. Kunhardt, Development of pulsed dielectric breakdown in liquids, Journal of Physics D: Applied Physics 28 (1) (1995) 178–188.
[10] M. Noskov, V. Kukhta, V. Lopatin, Simulation of the electric discharge development in inhomogeneous insulators, Journal of Physics D: Applied Physics 28 (1994) 1187–1194.
[11] D. Karpov, A. Kupershtokh, Models of streamer growth with "physical" time and fractal characteristics of streamer structures, in: Conference record 1998 IEEE Int. Symposium on Electrical Insulation, Arlington, VA, 1998, pp. 607–610.
[12] A. Kupershtokh, D. Karpov, Stochastic model of streamer growth in dielectric liquid with hydrodynamic expansion of streamer channels, in: Proc. 14th Int. Conf. on Dielectric Liquids, IEEE No. 02CH37319, Graz, Austria, 2002, pp. 111–114.
[13] N. Babaeva, G. Naidis, Modeling of positive streamers in liquid argon, Technical Physics Letters 25 (2) (1999) 91–94.
[14] A. Kupershtokh, D. Medvedev, Simulation of gas-dynamic flows during streamer propagation at liquid dielectrics breakdown, in: Conference record 1998 IEEE Int. Symposium on Electrical Insulation, Arlington, VA, 1998, pp. 611–614.
[15] L. D. Landau, E. M. Lifshitz, Electrodynamics of Continuous Media, Pergamon, Oxford, 1959.
[16] N. Yanenko, The method of fractional steps, Springer, Berlin, 1967.
[17] X. Shan, Simulation of Rayleigh–Bénard convection using a lattice Boltzmann method, Physical Review E 55 (3) (1997) 2780–2788.
[18] R. Zhang, H. Chen, Lattice Boltzmann method for simulations of liquid-vapor thermal flows, Physical Review E 67 (6) (2003) 066711.
[19] A. Kupershtokh, D. Medvedev, D. Karpov, On equations of state in a lattice Boltzmann method, Computers & Mathematics with Applications(in press).
[20] T. Lewis, A new model for the primary process of electrical breakdown in liquids, IEEE Transactions on Dielectrics and Electrical Insulation 5 (3) (1998) 306–315.